

# One-neutron stripping process in the $^{209}\text{Bi}(^{6}\text{Li}, ^{5}\text{Li})^{210}\text{Bi}^*$ reaction\*

Gao-Long Zhang,<sup>1</sup> Zhen-Wei Jiao,<sup>1</sup> Guang-Xin Zhang,<sup>2, †</sup> E. N. Cardozo,<sup>3</sup> B. Paes,<sup>4</sup> S. P. Hu,<sup>5, 6, ‡</sup> J. Q. Qian,<sup>1</sup> Daniele Mengoni,<sup>7, 8</sup> W. W. Qu,<sup>9</sup> C. B. Li,<sup>10</sup> Y. Zheng,<sup>10</sup> H. Q. Zhang,<sup>10</sup> H. B. Sun,<sup>5, 6</sup> N. Wang,<sup>5</sup> C. L. Zhang,<sup>11</sup> J. J. Valiente-Dobón,<sup>12</sup> D. Testov,<sup>8</sup> M. Mazzocco,<sup>7, 8</sup> A. Gozzelino,<sup>12</sup> C. Parascandolo,<sup>13</sup> D. Pierroutsakou,<sup>13</sup> M. La Commara,<sup>13, 14</sup> A. Goasduff,<sup>12</sup> D. Bazzacco,<sup>7</sup> D. R. Napoli,<sup>12</sup> F. Galtarossa,<sup>7</sup> F. Recchia,<sup>7, 8</sup> A. Illana,<sup>12</sup> S. Bakes,<sup>12</sup> I. Zanon,<sup>12</sup> S. Aydin,<sup>15</sup> G. de Angelis,<sup>12</sup> M. Siciliano,<sup>12, 16</sup> R. Menegazzo,<sup>7</sup> S. M. Lenzi,<sup>7, 8</sup> S. Akkoyun,<sup>17</sup> L. F. Canto,<sup>18</sup> and J. Lubian<sup>3, §</sup>

<sup>1</sup>School of Physics, Beihang University, 100191 Beijing, China

<sup>2</sup>Sino-French Institute of Nuclear Engineering and Technology, Sun Yat-Sen University, Zhuhai 519082, Guangdong, China

<sup>3</sup>Instituto de Física, Universidade Federal Fluminense, 24210-340, Niterói, Rio de Janeiro, Brazil

<sup>4</sup>Laboratorio TANDAR, Comisión Nacional de Energía Atómica, BKNA1650 San Martín, Argentina

<sup>5</sup>Institute for Advanced Study in Nuclear Energy & Safety, Shenzhen University, China

<sup>6</sup>Shenzhen Key Laboratory of Research and Manufacture of High Purity Germanium Materials and Detectors, Shenzhen University, 518060

<sup>7</sup>INFN, Sezione di Padova, Padova, Italy

<sup>8</sup>Dipartimento di fisica Astronomia dell'Università di Padova, Padova, Italy

<sup>9</sup>State Key Laboratory of Radiation Medicine and Protection,

School of Radiation Medicine and Protection, Soochow University, Suzhou 215123, China

<sup>10</sup>China Institute of Atomic Energy, Beijing 102413, China

<sup>11</sup>The Key Laboratory of Beam Technology and Material Modification of Ministry of Education, College of Nuclear Science and Technology, Beijing Normal University, Beijing 100875, China

<sup>12</sup>INFN, Laboratori Nazionali di Legnaro, I-35020 Legnaro, Italy

<sup>13</sup>INFN, Sezione di Napoli, I-80126 Napoli, Italy

<sup>14</sup>Dipartimento di Farmacia, Università di Napoli "Federico II", I-80131 Napoli, Italy

<sup>15</sup>Department of Natural and Mathematical Sciences, Faculty of Engineering, Tarsus University, 33480 Mersin, Turkey

<sup>16</sup>Physics Division, Argonne National Laboratory, Lemont-IL, USA

<sup>17</sup>Department of Physics, Sivas Cumhuriyet University, Sivas, Turkey

<sup>18</sup>Instituto de Física, Universidade Federal do Rio de Janeiro, CP 68528, 21941-972, Rio de Janeiro, Brazil

One-neutron stripping process between  $^6\text{Li}$  and  $^{209}\text{Bi}$  was studied at 28, 30, and 34 MeV using the in-beam  $\gamma$ -ray spectroscopy method. The  $\gamma$ - $\gamma$  coincident analysis clearly identified two  $\gamma$ -rays feeding the ground and long-lived isomeric states, which were employed to determine the cross section. The one-neutron stripping cross sections were similar to the cross sections of complete fusion in the  $^6\text{Li}+^{209}\text{Bi}$  system, but the one-neutron stripping cross sections decreased more gradually at the sub-barrier region. A coupled-reaction-channel calculation was performed to study the detailed reaction mechanism of the one-neutron stripping process in  $^6\text{Li}$ . The calculations indicated that the first excited state of  $^5\text{Li}$  is critical in the actual one-neutron transfer mechanism, and the valence proton of  $^{209}\text{Bi}$  can be excited to the low-lying excited state in  $(^6\text{Li}, ^5\text{Li})$  reaction, unlike in the (d,p) reaction.

Keywords: transfer reaction, weakly bound nuclei, cross section

## I. INTRODUCTION

In recent years, many theoretical and experimental works have focused on studying the reaction mechanism of weakly bound nuclei [1–13].  $^6\text{Li}$  is commonly utilized in experiments because of its  $\alpha+d$  cluster structure and low breakup threshold, resulting in complex reactions and diverse reaction mechanisms.

Because of the combined influence of Coulomb and nuclear interactions,  $^6\text{Li}$  might break up when approaching the target, giving rise to complete and incomplete fusion (CF and ICF) depending on whether all the projectile fragments are

captured or not. Besides, a transfer reaction is a process involving the direct transfer of one or more nucleons between the projectile and target.

The investigation of the coupling between the transfer and fusion processes has been a hot topic in recent years with a series of related publications [14–24].

The one-neutron stripping process in  $^6\text{Li}+^{96}\text{Zr}$  [14] and  $^6\text{Li}+^{89}\text{Y}$  [15] has been investigated to analyze the influence of transfer reaction on fusion. In both studies, it was concluded that the one-neutron stripping cross section has the same magnitude as the CF cross section around the Coulomb barrier and drops more gradually than the CF cross section in the sub-barrier region. Similar results were obtained in several other experiments, for instance, in  $^6\text{Li}+^{198}\text{Pt}$  [17],  $^7\text{Li}+^{198}\text{Pt}$  [18],  $^{6,7}\text{Li}+^{197}\text{Au}$  [19], and  $^{6,7}\text{Li}+^{64}\text{Zn}$  [20]. In the investigation of  $^9\text{Be}+^{169}\text{Tm}$ ,  $^{181}\text{Ta}$ ,  $^{187}\text{Re}$ , Fang et al. [21] quantitatively studied the relationship between the ratio of transfer to fusion cross section with the incident beam energy. The result showed that the ratio attained a value of 10 when the

\* Supported by the National Nature Science Foundation of China under Grants No. U2167204, No. 11975040, and No. 1832130.

† zhanggx3@mail.sysu.edu.cn

‡ husp@szu.edu.cn

§ jlubian@id.uff.br

beam energy was 10% lower than the barrier energy. Their research, along with the study in [25], has demonstrated that although the one-neutron transfer cross section holds significant importance in the sub-barrier region, its impact on the CF excitation function above the barrier is negligible.

The mechanism of (d,p) reactions, which is the most popular neutron-stripping reaction mechanism, is widely employed in the study of nuclear structure for the investigation of single-particle nature, spectroscopic factor, etc. [26–30]. For example, the (d,p) reaction was employed in  $^{120,124}\text{Sn}$  [31, 32],  $^{198}\text{Pt}$  [33], and  $^{96}\text{Zr}$  [34] targets to investigate the nuclear structure of  $^{121,125}\text{Sn}$ ,  $^{199}\text{Pt}$ , and  $^{97}\text{Zr}$ . In contrast, the same one-neutron transfer channel has been studied using  $(^6\text{Li}, ^5\text{Li})$  reactions, such as  $^{124}\text{Sn}(^6\text{Li}, ^5\text{Li})^{125}\text{Sn}$  [35],  $^{198}\text{Pt}(^6\text{Li}, ^5\text{Li})^{199}\text{Pt}$  [17],  $^{96}\text{Zr}(^6\text{Li}, ^5\text{Li})^{97}\text{Zr}$  [14], and  $^{120}\text{Sn}(^6\text{Li}, ^5\text{Li})^{121}\text{Sn}$  [22] reactions. These investigations mainly concentrated on the reaction cross section and the effect of transfer on the CF cross section.

$^6\text{Li}$  is commonly recognized as a cluster structure of  $\text{d}+\alpha$ . Assuming that  $\alpha$  does not participate in the neutron transfer process, the  $(^6\text{Li}, ^5\text{Li})$ , and (d,p) reactions are expected to have similar reaction mechanisms. Accordingly, when one finds discernible differences between two one-neutron transfer processes, such as the coupling between inelastic scattering and breakup, such investigations will shed light on the inner structure of the  $^6\text{Li}$ .

There are numerous researches on the level structure of  $^{210}\text{Bi}$  using (d,p) reaction [29, 30, 36–42], giving plenty of information on the different proton-neutron configurations; however, no information on the one-neutron stripping process in  $^6\text{Li}$  is available. In this work, the experimental result from the  $^6\text{Li}+^{209}\text{Bi}$  reaction has been elucidated, emphasizing the comparison with the (d,p) reaction.

This paper is organized into different sections as follows. Section II introduces the experimental setup and experimental details. The data analysis and experimental results are presented in Sec. III. Sec. IV demonstrates the theoretical model and the theoretical calculation process.

In Section V, we compare the CF cross section to the one-neutron transfer cross section and discuss the difference between the  $(^6\text{Li}, ^5\text{Li})$ , and (d,p) reactions. The summary is given in Sec. VI.

## II. EXPERIMENTAL SETUP

To obtain the one-neutron transfer cross sections of weakly bound nuclei with heavy target nuclei, the experiment of  $^6\text{Li}+^{209}\text{Bi}$  was performed at Legnaro National Laboratories (LNL), Italy. The profile of the experimental setup along the direction of incidence of the beam is shown in Fig. 1. A stable  $^6\text{Li}^{3+}$  beam with an average current intensity of 2.0 enA is produced by the Tandem-XTU accelerator. The  $^6\text{Li}$  beam energies are 28, 30, and 34 MeV, corresponding to 0.99, 1.06, and 1.21 times the height of the Coulomb barrier, respectively. A 550- $\mu\text{g}/\text{cm}^2$   $^{209}\text{Bi}$  target backed with a 110- $\mu\text{g}/\text{cm}^2$   $^{12}\text{C}$  foil is situated at the center of the detector array. The  $^{12}\text{C}$  foil is used to stop the residuals and eliminate

or minimize the Doppler effect of the observed  $\gamma$ -ray.

The GALILEO (Gamma detectors Array of Legnaro INFN Laboratories for nuclEar spectrOscopy) array was utilized to detect  $\gamma$ -rays emitted from various residuals. The GALILEO array is made up of 25 HPGe detectors spaced 235 mm apart from the target center and mounted on four support rings at different angles: 152° (5 detectors), 129° (5 detectors), 119° (5 detectors), and 90° (10 detectors). Additionally, each HPGe detector has an anti-Compton BGO crystal detector. The total measured full-energy-peak efficiency was 1.83% at 1408 keV. The energy resolution was 0.20% at 1408 keV transition of  $^{152}\text{Eu}$  calibration source (FWHM = 2.88 keV). In this experiment,  $\gamma$  ray energies detected by the GALILEO array range from 30 to 3000 keV.

At the center of the GALILEO array was the Si ball detection array known as EUCLIDES (EUrobAll Charged Light particle Identification DEtector Sphere). The 40 sets of 130- and 1000- $\mu\text{m}$ -thick  $\Delta\text{E-E}$  telescopes can perform charged particle discrimination.

To protect the Si detectors from the intense scattering particles, a cylindrical aluminum absorber of various thicknesses at different energies was placed in the EUCLIDES along the beam direction.

A Faraday cup (FC) was positioned 3 meters from the end of the beam to measure its intensity. The acquisition system in the experiment was an XDAQ-based, full digital acquisition system [43]. A more thorough explanation of the experimental setup is given in the references [44, 45].

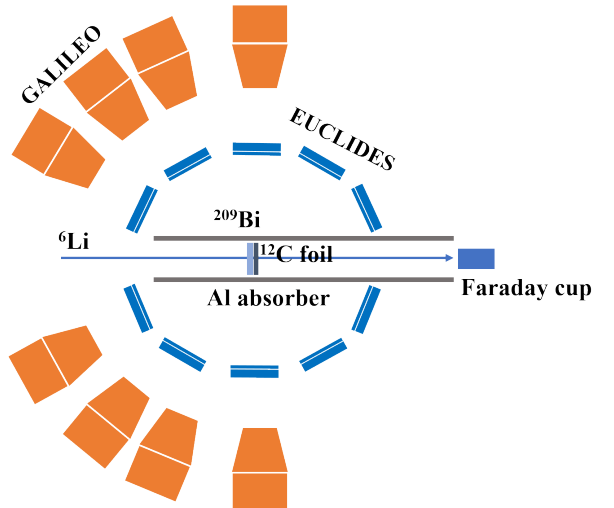


Fig. 1. Schematic of the experimental setup (sectional view). HPGe detectors and  $\Delta\text{E-E}$  telescopes present the schematic of a part of GALILEO and EUCLIDES arrays, respectively. For details, see the text.

## III. DATA ANALYSIS AND RESULTS

In the  $^6\text{Li}+^{209}\text{Bi}$  reaction, it is more challenging to evaporate charged particles than neutrons for a compound nucleus

(CN). Thus, the CN of the CF process,  $^{215}\text{Rn}$ , mainly decays by evaporating neutrons to form other lighter Rn isotopes. Similarly, the products of  $\alpha$ -ICF and d-ICF are mainly At and Po isotopes.

As a result, the  $^{210}\text{Bi}$  primarily originates from the one-neutron stripping process in this reaction system. This conclusion is also supported by the statistical evaporation code PACE4 [46].

The typical in-beam single- $\gamma$ -ray spectrum is displayed in Fig. 2 (a) at  $E_{\text{lab}}=30$  MeV. The  $\gamma$  transitions at 319.5 keV and 162.2 keV can be recognized clearly. Other rays in the spectrum are produced by  $^6\text{Li}$  reacting with the target  $^{209}\text{Bi}$  and the foil  $^{12}\text{C}$ , which include  $^{212}\text{Rn}$ ,  $^{210}\text{Po}$ ,  $^{209}\text{Po}$ , and  $^{13}\text{C}$ . Figures 2 (b) and (c) show the coincident spectra with a gate condition on the 319.5 and 162.2 keV transitions, respectively. The  $\gamma$  rays marked in the spectra can be found in the partial level scheme of  $^{210}\text{Bi}$ , as shown in Fig. 3. It should be mentioned here that all the levels belong to the identified multiplets organized by different proton-neutron configurations [29, 47] as shown in the same figure. This phenomenon implies that many excited states in  $^{210}\text{Bi}$  have been produced directly via the one-neutron stripping process. Because cross sections for high-lying levels are small, it is impossible to identify each one in the single  $\gamma$ -ray spectrum, and one can only obtain the cross section of the low-lying transitions, such as 319.5 and 162.2 keV  $\gamma$  rays.

The half-life of  $^{210}\text{Bi}$  ground state is 5.01 days, and a long-lived isomer state also exists with a half-life of  $3.04 \times 10^6$  years at 271.3 keV ( $9^-$  state).

In the current experiment, we add the intensities of the 319.5 and 162.2 keV transitions as the one neutron stripping partial cross sections, as shown in Table 1.

Table 1. Characteristic  $\gamma$  rays of  $^{210}\text{Bi}$  used to determine the one neutron transfer partial cross section.

Residual channels	Transition	$E\gamma$ (keV)	Feeding state
$^{210}\text{Bi}$	$2^- \rightarrow 1^-$	319.5	ground state
	$7^- \rightarrow 9^-$	162.2	long-lived isomer state

In the current work, the cross section for the one-neutron-stripping reaction is obtained as follows:

$$\sigma_{\text{one-neutron}}^*(E) = \frac{1}{N_B N_T} \left[ \sum_{i=1}^2 \frac{A_{E_{\gamma_i}} (1 + F_{E_{\gamma_i}})}{\varepsilon_{E_{\gamma_i}}} \right]. \quad (1)$$

Here,  $i = 1$  corresponds to the 319.5 keV transition and  $i = 2$  corresponds to the 162.2 keV transition.

$A_{E_{\gamma_i}}$  is the yield of the  $\gamma$  peak with energy  $E_{\gamma_i}$  at the bombarding energy  $E$ .  $\varepsilon_{E_{\gamma_i}}$  accounts for the absolute efficiency of all the detectors for the  $\gamma$ -ray with energy  $E_{\gamma_i}$ .

$F_{E_{\gamma_i}}$  is the inner conversion electron rate.  $N_B$  and  $N_T$  are the total number of beam particles incident on the target and the target atoms per unit area, respectively.

The uncertainties for the deduced cross section include: (1) the statistical error in  $\gamma$ -rays yield; (2) the error in the efficiency calibration of the detector, which is approximately

3%; and (3) error in the target thickness. The overall error bars range from 5% at  $E_{\text{beam}}=34$  MeV to approximately 10% at  $E_{\text{beam}}=28$  MeV. The result is summarized in Table 2.

#### IV. THEORETICAL ANALYSIS

The theoretical one-neutron stripping cross sections for the  $^{209}\text{Bi}(^6\text{Li}, ^5\text{Li})^{210}\text{Bi}^*$  reaction at 28, 30, and 34 MeV incident energies were obtained by performing coupled reaction channel (CRC) calculations using the Fresco code [48]. The optical potential used in the entrance partition ( $^6\text{Li}+^{209}\text{Bi}$ ) can be obtained from the elastic scattering. The experimental data of the elastic scattering obtained from Ref. [49] were studied. First, the standard São Paulo double folding potential (SPP) [50] was used as an optical potential in the real and imaginary parts ( $U = (1.0 + 0.78i)V_{SPP}$ ) in the optical model (OM) calculation. As observed in Fig. 4, the elastic angular distributions are not well described when SPP is used as the potential (dotted line). This is understandable because the systematic is only valid when there is no relevant coupling to the elastic channels. In this case, the coupling to the breakup channel should at least affect the angular distributions of the elastic scattering. Nonetheless, when SPP is used in the real part, and the Woods-Saxon imaginary potential, used in Ref. [49], is employed in the OM calculation, the data description is better (dashed line). However, for the CRC calculation, the coupling of the inelastic scattering states of  $^{209}\text{Bi}$  and the transfer channel were explicitly included (red line). Therefore, it was necessary to reduce the depth of the imaginary potential to avoid double counting and consider the loss of flux to other channels. Thus, the depth of the imaginary part was reduced by 10 MeV in each energy, keeping the radius and diffusivity fixed. One can note that the inelastic scattering and transfer channels slightly influence the elastic scattering. For the energies of 28 and 30 MeV, the elastic distributions suffered a slight increase, while the cross section decreased for 34 MeV when compared with the results of the OM calculation, which considered only the ground states of each nucleus in the entrance partition. This behavior at the highest energy was anticipated ( $E > V_B$ ) because the couplings to breakup channels were not included. It is well known that these dynamic couplings produce repulsive polarization potentials that increase  $V_B$  and hinder the CF fusion cross section, especially at energies above  $V_B$  [5, 51, 52]. Consequently, the elastic scattering should increase with a decrease in fusion.

The single-particle wave functions were derived using Woods-Saxon potentials for the nuclear interactions in the intrinsic Hamiltonian. Standard reduced radius  $r_0 = 1.25$  fm and diffuseness  $a = 0.65$  fm were used to generate the single-particle wave functions for the target and projectile nuclei. The potential depths were varied to fit the experimental one-neutron separation energies.

The coupling scheme for the current calculation is shown in Fig. 5, which depicts the rays cascading with the 319.5 or 162.2 keV transitions. Since the  $^{209}\text{Bi}$  had 83 protons and 126 neutrons, the last valence proton could occupy  $\pi$  ( $h_{9/2}$ ,  $f_{7/2}$ , or  $i_{13/2}$ ) orbitals, giving rise to the configuration of the

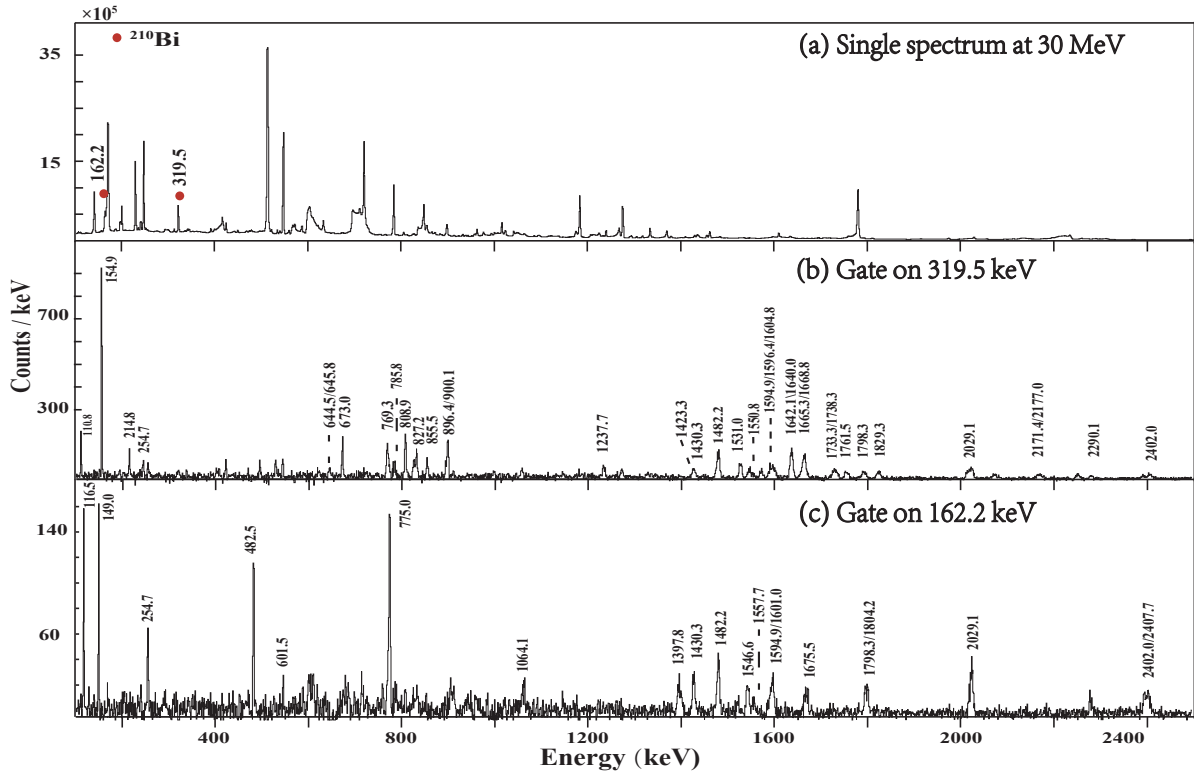


Fig. 2. (a) Typical in-beam  $\gamma$ -ray spectrum depicting the  $\gamma$  lines of the one neutron stripping residue nucleus  $^{210}\text{Bi}$  in the  $^6\text{Li} + ^{209}\text{Bi}$  system at the bombarding energy of 30 MeV. Panels (b) and (c) show the coincident spectra of the 319.5 and 162.2 keV transitions, respectively.

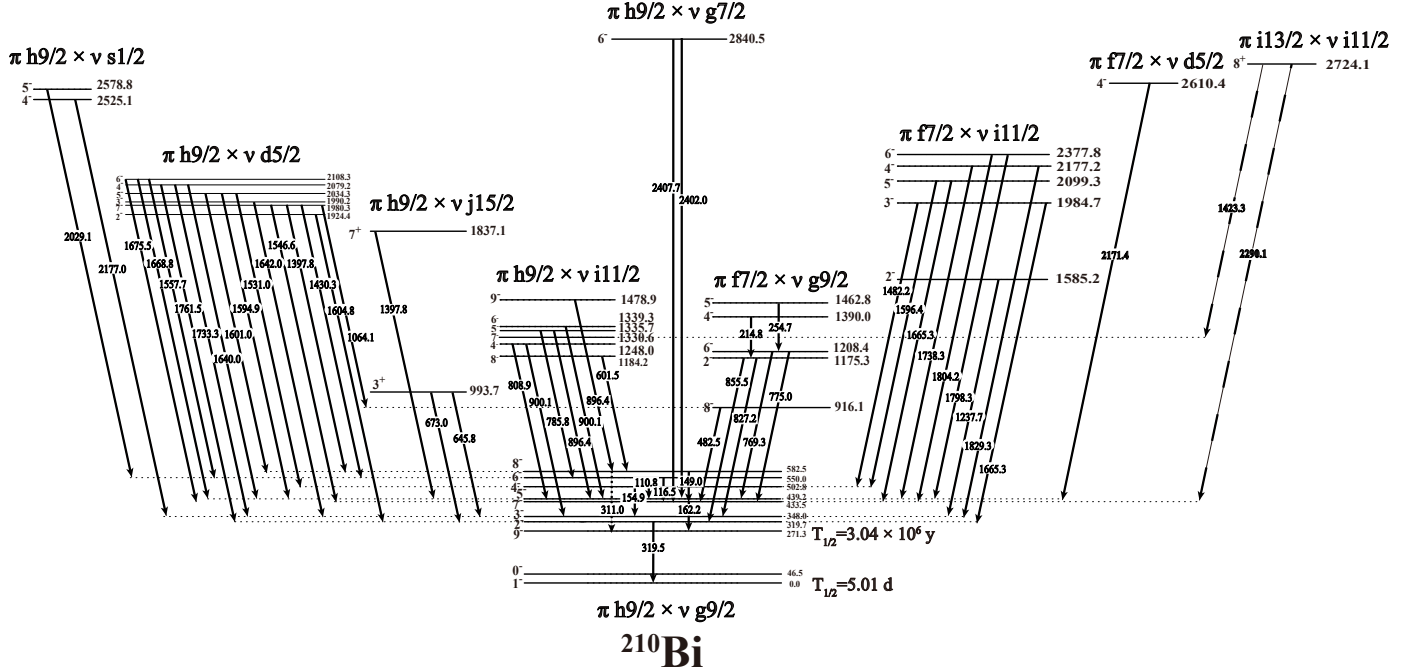


Fig. 3. Partial level scheme of  $^{210}\text{Bi}$  in the unit of keV. The configuration information is mainly referred from [29, 47].

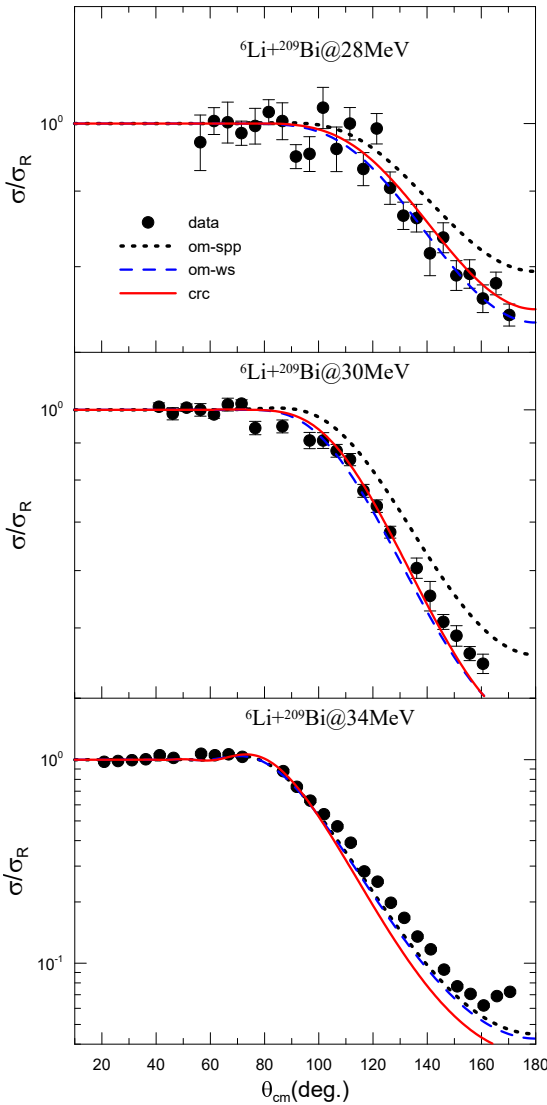


Fig. 4. (color online) Elastic scattering angular distribution, for the  ${}^6\text{Li} + {}^{209}\text{Bi}$  at 28, 30, and 34 MeV, obtained from OM and CRC calculations. The elastic scattering data were extracted from [49].

ground state and two lowest excited states in  ${}^{209}\text{Bi}$  [53]. Because of the fact that during the one-neutron stripping reaction, the valence neutron might be added to all the possible empty orbitals outside the  $N = 126$  shell, including  $\nu$  ( $\text{g}_{9/2}$ ,  $\text{i}_{11/2}$ ,  $\text{j}_{15/2}$ ,  $\text{d}_{5/2}$ ,  $\text{s}_{1/2}$ , and  $\text{g}_{7/2}$ ), different multiplets with similar strengths would be produced. According to the aforementioned  $\gamma$ - $\gamma$  coincidence analysis, even though low, almost all the multiplets (or part of the members) with valence proton on both  $\pi 1\text{h}_{9/2}$  or  $2\text{f}_{7/2}$  orbitals are clearly observed. Multiplets with protons on  $\pi 1\text{l}_{13/2}$  orbital have also been found, but their existence is uncertain because of very weak intensity and the interference of the same energy  $\gamma$  rays. Therefore, the coupling of this orbit is indicated by dashed lines in Fig. 5, emphasizing its uncertainty. This is the coupling originating from the first and second excited states in  ${}^{209}\text{Bi}$  must be con-

sidered in the current calculation.

As a result, the levels whose decay transitions have a cascade relationship with the two observed  $\gamma$  rays up to approximately 3000 keV, corresponding to the  $(\text{h}_{9/2}^\pi \otimes \text{g}_{9/2}^\nu)$ ,  $(\text{f}_{7/2}^\pi \otimes \text{g}_{9/2}^\nu)$ ,  $(\text{h}_{9/2}^\pi \otimes \text{i}_{11/2}^\nu)$ ,  $(\text{h}_{9/2}^\pi \otimes \text{j}_{15/2}^\nu)$ ,  $(\text{h}_{9/2}^\pi \otimes \text{d}_{5/2}^\nu)$ ,  $(\text{f}_{7/2}^\pi \otimes \text{i}_{11/2}^\nu)$ ,  $(\text{h}_{9/2}^\pi \otimes \text{s}_{1/2}^\nu)$ ,  $(\text{f}_{7/2}^\pi \otimes \text{d}_{5/2}^\nu)$ ,  $(\text{h}_{9/2}^\pi \otimes \text{g}_{7/2}^\nu)$ , and  $(\text{i}_{13/2}^\pi \otimes \text{i}_{11/2}^\nu)$  configurations, are considered in the current calculation.

The one-neutron spectroscopic amplitudes for target overlaps were derived from shell-model calculations using the NuShellX code [54]. The  $khpe$  effective phenomenological interaction [55, 56] was used to describe the structure of the target and the residual nucleus. The model space assumes  ${}^{208}\text{Pb}$  as a closed core with  $1\text{h}_{9/2}$ ,  $2\text{f}_{7/2}$ ,  $2\text{f}_{5/2}$ ,  $3\text{p}_{3/2}$ ,  $3\text{p}_{1/2}$ , and  $1\text{i}_{13/2}$  orbitals as valence space for protons, and  $1\text{i}_{11/2}$ ,  $2\text{g}_{9/2}$ ,  $2\text{g}_{7/2}$ ,  $3\text{d}_{5/2}$ ,  $3\text{d}_{3/2}$ ,  $4\text{s}_{1/2}$ , and  $1\text{j}_{15/2}$  for neutrons. Because of our computational limitations in performing shell-model calculations, it was necessary to introduce some constraints to derive the amplitudes using these large valence spaces. Therefore, the last valence orbitals for protons and neutrons were constrained so that only two nucleons could occupy them.

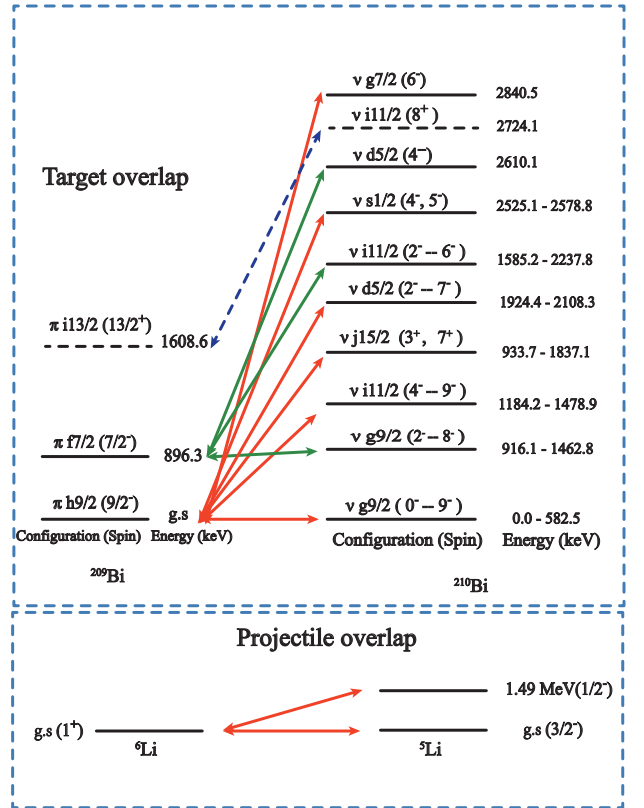


Fig. 5. (color online) Coupling scheme considered for projectile and target overlaps in the  ${}^{209}\text{Bi}({}^6\text{Li}, {}^5\text{Li}){}^{210}\text{Bi}$  reaction.

The experimental measurements in this paper reported counts for two  $\gamma$ -rays: the 319.5 keV and 162.2 keV electromagnetic transitions in the residual nucleus  ${}^{210}\text{Bi}$  from

the one-neutron stripping reaction. However, the cross sections were contributed by both the de-excitations from the highly excited states and the direct population of the  $2_{0.319}^-$  and  $7_{0.433}^-$  states of  $^{210}\text{Bi}$ . The sum of the contributions of channels that decay through  $\gamma$ -transitions of 319.5 keV and 162.2 keV and the resulting integrated one-neutron transfer cross-sections are shown in Table 2.

## V. DISCUSSION

In fact,  $^5\text{Li}$  is an unbound nucleus that decays in  $^4\text{He} + p$ . Concerning the  $\langle ^6\text{Li}|^5\text{Li} \rangle$  overlap we are considering the first step in the CRC calculations, forming the  $^5\text{Li}$  g.s. resonance, and then decaying. It is enough for the resonance to survive for a reasonable time. In these cases, this state can be considered as a bound state in CC calculations. This is a typical procedure in CC calculations to describe thick resonances like the  $^{6,7}\text{Li}$  resonances [5]. The  $^5\text{Li}$   $1/2^-$  resonance was also considered as a bound state.

As shown in Table 2, when the spectroscopic amplitude of the projectile overlaps was set to 1.0, many calculations were carried out to evaluate the effects of the excited states of  $^{209}\text{Bi}$  and  $^5\text{Li}$  on the cross section. The first one considers only the ground state of  $^5\text{Li}$  ( $3/2^-$ ), and the results are designated as CS1, CS3, and CS5, respectively. Among these, CS1 considers the ground state as well as two excited states of  $^{209}\text{Bi}$ , CS5 considers both the ground state and the first excited state, and CS3 only considers the ground state. Furthermore, the first resonant state of  $^5\text{Li}$  ( $1/2^-$ ) is considered, and the results are labeled CS2 and CS4. Similarly, CS2 studies  $^{209}\text{Bi}$ 's ground state as well as two low excited states, but CS4 only considers the ground state. By comparing CS1 with CS2, the cross sections calculated considering the first resonance state of  $^5\text{Li}$  are approximately 22% (at 28 MeV)—39% (at 34 MeV) higher than that calculated when only considering the ground state of  $^5\text{Li}$ .

The results suggest that the first excited state of  $^5\text{Li}$  is critical in the actual one-neutron transfer mechanism. The underlying theory and physics should be explored further in future works.

When comparing the results of the experimental integral cross section and the theoretical calculation in CS2, which considers both the excited states of  $^{209}\text{Bi}$  and  $^5\text{Li}$ , the two cross sections are in good agreement when the beam energy is 28 MeV. At 30 MeV, the theoretical calculation overestimates the cross section, and at 34 MeV, the experimental results are higher than that of the theoretical calculation. The discrepancies between the calculated and experimental cross sections indicate that the refined spectroscopic amplitudes must be considered in further calculations to make the theoretical and experimental results match better.

When comparing CS1, CS3, and CS5, we can observe that the effect on the integrated cross section is not noticeable after accounting for the first and second excited states of  $^{209}\text{Bi}$ . This indicates that  $^{209}\text{Bi}$  was excited during the transfer reaction, but its effect on the transfer cross section was negligible.

It is known that the (d,p) reaction is frequently employed

to investigate the single-particle nature of different states in the produced nucleus. Levels in  $^{210}\text{Bi}$  have been studied by the  $^{209}\text{Bi}(\text{d},\text{p})^{210}\text{Bi}$  reaction at 19 MeV and the  $^{209}\text{Bi}(\alpha,^3\text{He})^{210}\text{Bi}$  reaction at 58 MeV [29]. In this study, the observed energy levels are interpreted as the multiplets formed by coupling a valence proton occupying the  $1\text{h}_{9/2}$  orbital, with a neutron in either  $2\text{g}_{9/2}$ ,  $1\text{i}_{11/2}$ ,  $1\text{j}_{15/2}$ ,  $3\text{d}_{5/2}$ ,  $4\text{s}_{1/2}$ ,  $2\text{g}_{7/2}$ , or  $3\text{d}_{3/2}$  orbitals [29, 47]. Note here that the ground state in  $^{209}\text{Bi}$  has a spin-parity of  $9/2^-$ , being identified as a single-proton configuration ( $\text{h}_{9/2}$ ). This means the deuteron does not excite the target nucleus during the one-neutron stripping process, being suitable for the study of transferred momentum, spectroscopic factor, or other observables, which can reflect the single-particle nature of the produced levels in the existing channel. However, in the case of  $^6\text{Li}$ , in addition to  $\pi \text{h}_{9/2}$ , the observed level scheme as shown in Fig. 3 also includes the excited states with valence protons in  $2\text{f}_{7/2}$  and  $1\text{i}_{13/2}$  orbitals. Thus,  $^6\text{Li}$  can significantly excite the  $^{209}\text{Bi}$  target during the one-neutron process.

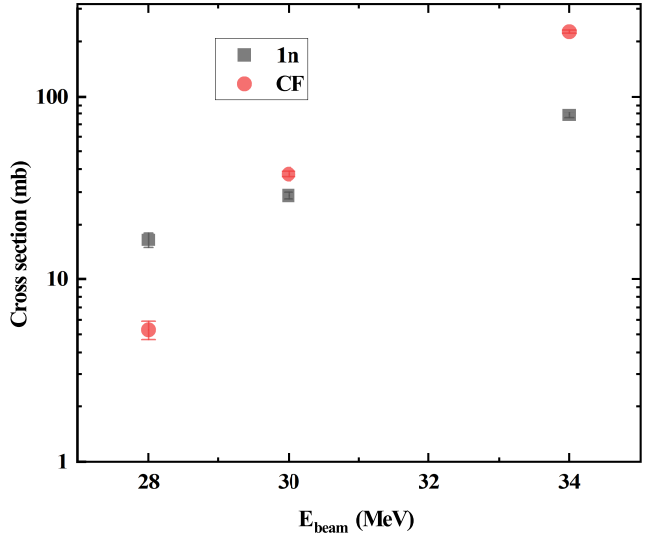


Fig. 6. Comparison of cross sections for the one-neutron stripping reaction and the CF reaction in the  $^6\text{Li}+^{209}\text{Bi}$  reaction system. The CF cross sections are taken from [5]

In Fig. 6, the cross sections of the one-neutron stripping reaction and the CF [5] are compared in the  $^6\text{Li}+^{209}\text{Bi}$  system.

When the beam energy decreases, the cross section of the one-neutron stripping process gradually exceeds that of the CF reaction, being quite similar to the case of  $^6\text{Li}+^{96}\text{Zr}$  [14]. This behavior is commonly explained by the fact that the neutron transfer does not need to overcome the Coulomb barrier, being different from the CF process.

Meanwhile, the coupling between the neutron-stripping and the fusion process is still under investigation.

Table 2. Comparison of the one-neutron integrated cross-section considering the spectroscopic amplitude for projectile overlap set to 1.0. Different columns indicate that different excited and ground states of  ${}^5\text{Li}$  and  ${}^{209}\text{Bi}$  are considered, as described in detail in the text.

E (MeV)	CS <sub>Exp</sub> (mb)	CS1 <sub>Theo</sub> (mb)	CS2 <sub>Theo</sub> (mb)	CS3 <sub>Theo</sub> (mb)	CS4 <sub>Theo</sub> (mb)	CS5 <sub>Theo</sub> (mb)
state of ${}^{209}\text{Bi}$		g.s+f <sub>7/2</sub> +i <sub>13/2</sub>	g.s+f <sub>7/2</sub> +i <sub>13/2</sub>	g.s	g.s	g.s+f <sub>7/2</sub>
state of ${}^5\text{Li}$		g.s	g.s+p <sub>1/2</sub>	g.s	g.s+p <sub>1/2</sub>	g.s
28	16.41 $\pm$ 1.71	13.77	16.86	13.61	16.85	13.77
30	28.81 $\pm$ 1.53	26.70	35.84	26.74	34.77	26.70
34	79.23 $\pm$ 4.20	47.49	66.15	47.41	68.41	47.41

## VI. SUMMARY

Experiments on the  ${}^6\text{Li}+{}^{209}\text{Bi}$  reaction were performed on the GALILEO Array coupled with  $4\pi$  Si-ball EUCLIDES at Legnaro National Laboratory to study the transfer of weakly bound nuclei on heavy target nuclei in the near-barrier energy region. The one-neutron stripping product  ${}^{210}\text{Bi}$  populates the excited state, and the de-excited rays are identified by using the  $\gamma$ - $\gamma$  coincidence method. The yield of  ${}^{210}\text{Bi}$  is calculated via two rays, 319.5 keV and 162.2 keV, which are de-excited to the ground and the long-lived states, respectively.

The one-neutron stripping partial cross sections obtained at 28, 30, and 34 MeV are comparable to those obtained for CF. As incident energy decreases, the excitation function for the one-neutron transfer reaction decreases more slowly. It exceeds the fusion section at energies below the Coulomb barrier. This indicates that the one-neutron transfer reaction plays a more important role in the reaction systems involving weakly bound nuclei at energies around and below the Coulomb barrier.

The theoretical one-neutron transfer cross sections were obtained by performing CRC calculations. The cross sections calculated considering the first excited state of  ${}^5\text{Li}$  are approximately 20% to 40% larger than those calculated considering only the ground state of  ${}^5\text{Li}$ . Furthermore, in contrast to the (d,p) reaction, the valence proton of  ${}^{209}\text{Bi}$  is excited to the low-lying states in  $({}^6\text{Li}, {}^5\text{Li})$  reaction, implying that the single-particle energy level of  ${}^{210}\text{Bi}$  cannot be studied using this reaction.

## ACKNOWLEDGMENTS

We are grateful to the INFN-LNL staff for providing a stable  ${}^6\text{Li}$  beam throughout the experiment. This work is supported by the National Nature Science Foundation of China under Grant Nos. U2167204, 11975040, and 1832130. The work supported in part by the Brazilian funding agencies CAPES, CNPq, FAPERJ, and the INCT-FNA (Instituto Nacional de Ciéncia e Tecnologia- Física Nuclear e Aplicações), research project 464898/2014-5. S. P. Hu was supported by Guang dong Key Research And Development Program No. 2020B040420005, Guang dong Basic and Applied Basic Research Foundation No. 2021B1515120027, Ling Chuang Re-

search Project of China National Nuclear Corporation No. 20221024000072F6-0002-7, and Nuclear Energy Development and Research Project No. HNKF202224(28). The work was also supported by the '111' center (B20065). M. Siciliano was supported by the U.S. Department of Energy, Office of Science, Office of Nuclear Physics, under contract number DE-AC02- 06CH1135.

[1] B.B. Back, H. Esbensen, C.L. Jiang et al., Recent developments in heavy-ion fusion reactions. *Rev. Mod. Phys.* **86**, 317–360 (2014). [doi:10.1103/RevModPhys.86.317](https://doi.org/10.1103/RevModPhys.86.317)

[2] C. Beck, N. Keeley, A. Diaz-Torres, Coupled-channel effects in elastic scattering and near-barrier fusion induced by weakly bound nuclei and exotic halo nuclei. *Phys. Rev. C* **75**, 054605 (2007). [doi:10.1103/PhysRevC.75.054605](https://doi.org/10.1103/PhysRevC.75.054605)

[3] L. Canto, P. Gomes, R. Donangelo et al., Fusion and breakup of weakly bound nuclei. *Phys. Rep.* **424**, 1–111 (2006). [doi:https://doi.org/10.1016/j.physrep.2005.10.006](https://doi.org/10.1016/j.physrep.2005.10.006)

[4] L. Canto, P. Gomes, R. Donangelo et al., Recent developments in fusion and direct reactions with weakly bound nuclei. *Phys. Rep.* **596**, 1–86 (2015). [doi:https://doi.org/10.1016/j.physrep.2015.08.001](https://doi.org/10.1016/j.physrep.2015.08.001)

[5] M. Dasgupta, P.R.S. Gomes, D.J. Hinde et al., Effect of breakup on the fusion of  $^6\text{Li}$ ,  $^7\text{Li}$ , and  $^9\text{Be}$  with heavy nuclei. *Phys. Rev. C* **70**, 024606 (2004). [doi:10.1103/PhysRevC.70.024606](https://doi.org/10.1103/PhysRevC.70.024606)

[6] N. Keeley, N. Alamanos, K. Kemper et al., Elastic scattering and reactions of light exotic beams. *Prog. Part. Nucl. Phys.* **63**, 396–447 (2009). [doi:https://doi.org/10.1016/j.ppnp.2009.05.003](https://doi.org/10.1016/j.ppnp.2009.05.003)

[7] N. Keeley, R. Raabe, N. Alamanos et al., Fusion and direct reactions of halo nuclei at energies around the coulomb barrier. *Prog. Part. Nucl. Phys.* **59**, 579–630 (2007). [doi:https://doi.org/10.1016/j.ppnp.2007.02.002](https://doi.org/10.1016/j.ppnp.2007.02.002)

[8] K. Hagino, N. Takigawa, Subbarrier Fusion Reactions and Many-Particle Quantum Tunneling. *Prog. Theor. Phys.* **128**, 1061–1106 (2012). [doi:10.1143/PTP.128.1061](https://doi.org/10.1143/PTP.128.1061)

[9] J.F. Liang, C. Signorini, Fusion induced by radioactive ion beams. *Int. J. Mod. Phys. E* **14**, 1121–1150 (2005).

[10] C.S. Palshetkar, S. Santra, A. Chatterjee et al., Fusion of the weakly bound projectile  $^9\text{Be}$  with  $^{89}\text{Y}$ . *Phys. Rev. C* **82**, 044608 (2010). [doi:10.1103/PhysRevC.82.044608](https://doi.org/10.1103/PhysRevC.82.044608)

[11] S. Santra, V. Parkar, K. Ramachandran et al., Resonant breakup of  $^6\text{Li}$  by  $^{209}\text{Bi}$ . *Phys. Lett. B* **677**, 139–144 (2009). [doi:https://doi.org/10.1016/j.physletb.2009.05.016](https://doi.org/10.1016/j.physletb.2009.05.016)

[12] A. Shrivastava, A. Navin, A. Lemasson et al., Exploring fusion at extreme sub-barrier energies with weakly bound nuclei. *Phys. Rev. Lett.* **103**, 232702 (2009). [doi:10.1103/PhysRevLett.103.232702](https://doi.org/10.1103/PhysRevLett.103.232702)

[13] G.L. Zhang, C.L. Zhang, H.Q. Zhang et al., Quasi-elastic scattering of the proton drip line nucleus  $^{17}\text{f}$  on  $^{12}\text{c}$  at 60 mev. *Eur. Phys. J. A* **48**, 65 (2012). [doi:10.1140/epja/i2012-12065-x](https://doi.org/10.1140/epja/i2012-12065-x)

[14] S.P. Hu, G.L. Zhang, J.C. Yang et al., One-neutron stripping processes to excited states of the  $^6\text{Li} + ^{96}\text{Zr}$  reaction at near-barrier energies. *Phys. Rev. C* **93**, 014621 (2016). [doi:10.1103/PhysRevC.93.014621](https://doi.org/10.1103/PhysRevC.93.014621)

[15] G.L. Zhang, G.X. Zhang, S.P. Hu et al., One-neutron stripping processes to excited states of  $^{90}\text{Y}^*$  in the  $^{89}\text{Y} (^6\text{Li}, ^5\text{Li}) ^{90}\text{Y}^*$  reaction. *Phys. Rev. C* **97**, 014611 (2018). [doi:10.1103/PhysRevC.97.014611](https://doi.org/10.1103/PhysRevC.97.014611)

[16] Y.D. Fang, P.R.S. Gomes, J. Lubian et al., One-neutron stripping from  $^9\text{Be}$  to  $^{169}\text{Tm}$ ,  $^{181}\text{Ta}$ , and  $^{187}\text{Re}$  at near-barrier energies. *Phys. Rev. C* **93**, 034615 (2016). [doi:10.1103/PhysRevC.93.034615](https://doi.org/10.1103/PhysRevC.93.034615)

[17] A. Shrivastava, A. Navin, A. Lemasson et al., Exploring fusion at extreme sub-barrier energies with weakly bound nuclei. *Phys. Rev. Lett.* **103**, 232702 (2009). [doi:10.1103/PhysRevLett.103.232702](https://doi.org/10.1103/PhysRevLett.103.232702)

[18] A. Shrivastava, A. Navin, A. Diaz-Torres et al., Role of the cluster structure of  $^7\text{Li}$  in the dynamics of fragment capture. *Phys. Lett. B* **718**, 931–936 (2013). [doi:https://doi.org/10.1016/j.physletb.2012.11.064](https://doi.org/10.1016/j.physletb.2012.11.064)

[19] C.S. Palshetkar, S. Thakur, V. Nanal et al., Fusion and quasi-elastic scattering in the  $^6,^7\text{Li} + ^{197}\text{Au}$  systems. *Phys. Rev. C* **89**, 024607 (2014). [doi:10.1103/PhysRevC.89.024607](https://doi.org/10.1103/PhysRevC.89.024607)

[20] A. Di Pietro, P. Figuera, E. Strano et al., Heavy residue excitation functions for the collisions  $^6,^7\text{Li} + ^{64}\text{Zn}$  near the coulomb barrier. *Phys. Rev. C* **87**, 064614 (2013). [doi:10.1103/PhysRevC.87.064614](https://doi.org/10.1103/PhysRevC.87.064614)

[21] Y.D. Fang, P.R.S. Gomes, J. Lubian et al., Complete and incomplete fusion of  $^9\text{Be} + ^{169}\text{Tm}$ ,  $^{187}\text{Re}$  at near-barrier energies. *Phys. Rev. C* **91**, 014608 (2015). [doi:10.1103/PhysRevC.91.014608](https://doi.org/10.1103/PhysRevC.91.014608)

[22] M. Fisichella, A.C. Shotter, P. Figuera et al., Breakup and  $n$ -transfer effects on the fusion reactions  $^6,^7\text{Li} + ^{120,119}\text{Sn}$  around the coulomb barrier. *Phys. Rev. C* **95**, 034617 (2017). [doi:10.1103/PhysRevC.95.034617](https://doi.org/10.1103/PhysRevC.95.034617)

[23] M.K. Pradhan, A. Mukherjee, S. Roy et al., Importance of the  $1n$ -stripping process in the  $^6\text{Li} + ^{159}\text{Tb}$  reaction. *Phys. Rev. C* **88**, 064603 (2013). [doi:10.1103/PhysRevC.88.064603](https://doi.org/10.1103/PhysRevC.88.064603)

[24] S. Santra, S. Kailas, V.V. Parkar et al., Disentangling reaction mechanisms for  $\alpha$  production in the  $^6\text{Li} + ^{209}\text{Bi}$  reaction. *Phys. Rev. C* **85**, 014612 (2012). [doi:10.1103/PhysRevC.85.014612](https://doi.org/10.1103/PhysRevC.85.014612)

[25] P.R.S. Gomes, A.M.M. Maciel, R.M. Anjos et al., Transfer reactions as a doorway to fusion. *J. Phys. G: Nucl. Part. Phys.* **23**, 1315 (1997). [doi:10.1088/0954-3899/23/10/020](https://doi.org/10.1088/0954-3899/23/10/020)

[26] N. Timofeyuk, R. Johnson, Theory of deuteron stripping and pick-up reactions for nuclear structure studies. *Prog. Part. Nucl. Phys.* **111**, 103738 (2020). [doi:https://doi.org/10.1016/j.ppnp.2019.103738](https://doi.org/10.1016/j.ppnp.2019.103738)

[27] S. Butler, On angular distributions from (d,p) and (d,n) nuclear reactions [2]. *Phys. Rev.* **80**, 1095 – 1096 (1950). [doi:10.1103/PhysRev.80.1095.2](https://doi.org/10.1103/PhysRev.80.1095.2)

[28] K. Wimmer, Nucleon transfer reactions with radioactive beams. *J. Phys. G: Nucl. Part. Phys.* **45**, 033002 (2018). [doi:10.1088/1361-6471/aaa2bf](https://doi.org/10.1088/1361-6471/aaa2bf)

[29] C. Cline, W. Alford, H. Gove et al., Multiplet structure of  $^{210}\text{Bi}$  from the  $^{209}\text{Bi}(d, p)$  and  $^{209}\text{Bi}(\alpha, ^3\text{He})$  reactions. *Nucl. Phys. A* **186**, 273–296 (1972). [doi:https://doi.org/10.1016/0375-9474\(72\)90046-2](https://doi.org/10.1016/0375-9474(72)90046-2)

[30] J.J. Kolata, W.W. Daehnick, Shell-model structure of  $^{210}\text{Bi}$ :  $^{209}\text{Bi}(d, p)$  at 17 mev. *Phys. Rev. C* **5**, 568–578 (1972). [doi:10.1103/PhysRevC.5.568](https://doi.org/10.1103/PhysRevC.5.568)

[31] C.R. Bingham, D.L. Hillis, Neutron shell structure in  $^{125}\text{Sn}$  by  $(d, p)$  and  $(\alpha, ^3\text{He})$  reactions. *Phys. Rev. C* **8**, 729–736 (1973). [doi:10.1103/PhysRevC.8.729](https://doi.org/10.1103/PhysRevC.8.729)

[32] M.J. Bechara, O. Dietzsch, States in  $^{121}\text{Sn}$  from the  $^{120}\text{Sn}(d, p)^{121}\text{Sn}$  reaction at 17 mev. *Phys. Rev. C* **12**, 90–101 (1975). [doi:10.1103/PhysRevC.12.90](https://doi.org/10.1103/PhysRevC.12.90)

[33] D. Burke, G. Kajrys, Single-nucleon-transfer tests of the  $u(612)$  supersymmetry in platinum isotopes. *Nucl. Phys. A* **517**, 1–26 (1990). [doi:https://doi.org/10.1016/0375-9474\(90\)90258-N](https://doi.org/10.1016/0375-9474(90)90258-N)

[34] C.R. Bingham, G.T. Fabian, Neutron shell structure in  $^{93}\text{Zr}$ ,  $^{95}\text{Zr}$ , and  $^{97}\text{Zr}$  by  $(d, p)$  and  $(\alpha, ^3\text{He})$  reactions. *Phys. Rev. C* **7**, 1509–1518 (1973). [doi:10.1103/PhysRevC.7.1509](https://doi.org/10.1103/PhysRevC.7.1509)

[35] V.V. Parkar, A. Parmar, P. M. et al., Investigating neutron transfer in the  $^6\text{Li} + ^{124}\text{Sn}$  system. *Phys. Rev. C* **107**, 024602 (2023). [doi:10.1103/PhysRevC.107.024602](https://doi.org/10.1103/PhysRevC.107.024602)

[36] J.R. Erskine, W.W. Buechner, H.A. Enge,  $^{209}\text{Bi}$  (d, p)  $^{210}\text{Bi}$  reaction at low bombarding energies and with high resolution. *Phys. Rev* **128**, 720 (1962).

[37] C. Ellegaard, P.D. Barnes, R. Eisenstein et al., Decay modes and lifetimes of the levels in the  $\pi h92 \cdot \nu g92$  multiplet in  $^{210}\text{Bi}$ . *Phys. Lett. B* **35**, 145–147 (1971).

[38] H.T. Motz, E.T. Journey, E.B. Shera et al., Low-lying configurations in  $^{210}\text{Bi}$ . *Phys. Rev. Lett.* **26**, 854 (1971).

[39] C.V.K. Baba, T. Faestermann, D.B. Fossan et al., Magnetic moments of the 7- and 5-( $\pi$  h 9/2,  $\nu$  g 9/2) states in  $^{210}\text{Bi}$ . *Phys. Rev. Lett.* **29**, 496 (1972).

[40] D. Proetel, F. Riess, E. Grosse et al., Gamma decay of excited states in  $^{210}\text{Bi}$  and an interpretation with the shell model. *Phys. Rev. C* **7**, 2137 (1973).

[41] D.J. Donahue, O. Häusser, R.L. Hershberger et al., Transition rates between two-body states in  $^{206}\text{Tl}$ ,  $^{208}\text{Bi}$ , and  $^{210}\text{Bi}$ . *Phys. Rev. C* **12**, 1547 (1975).

[42] T.R. Canada, R.A. Eisenstein, C. Ellegaard et al., The  $\gamma$ -decay of two-particle states in  $^{210}\text{Bi}$ . *Nucl. Phys. A* **205**, 145–167 (1973).

[43] J. Guteleber, S. Murray, L. Orsini, Towards a homogeneous architecture for high-energy physics data acquisition systems. *Comput. Phys. Commun.* **153**, 155–163 (2003). [doi:  
https://doi.org/10.1016/S0010-4655\(03\)00161-9](https://doi.org/10.1016/S0010-4655(03)00161-9)

[44] A. Goasduff, D. Mengoni, F. Recchia et al., The galileo -ray array at the legnaro national laboratories. *Nucl. Instr. and Meth. Phys. Res. A* **1015**, 165753 (2021). [doi:  
https://doi.org/10.1016/j.nima.2021.165753](https://doi.org/10.1016/j.nima.2021.165753)

[45] D. Testov, D. Mengoni, A. Goasduff et al., The 4  $\pi$  highly-efficient light-charged-particle detector euclides, installed at the galileo array for in-beam  $\gamma$ -ray spectroscopy. *Eur. Phys. J. A* **55**, 47 (2019). [doi:  
https://doi.org/https://doi.org/geant4.web.cern.ch/](https://doi.org/https://doi.org/geant4.web.cern.ch/)

[46] A. Gavron, Statistical model calculations in heavy ion reactions. *Phys. Rev. C* **21**, 230–236 (1980).

[47] R.K. Sheline, R.L. Ponting, A.K. Jain et al., Spectroscopy of the high-lying configurations in  $^{210}\text{Bi}$ . *Czech.J.Phys.* **39**, 22 (1989). [doi:  
https://doi.org/10.1007/BF01597435](https://doi.org/10.1007/BF01597435)

[48] I.J. Thompson, Coupled reaction channels calculations in nuclear physics. *Comput. Phys. Rep.* **7**, 167–212 (1988). [doi:  
https://doi.org/10.1016/0167-7977\(88\)90005-6](https://doi.org/10.1016/0167-7977(88)90005-6)

[49] S. Santra, S. Kailas, K. Ramachandran et al., Reaction mechanisms involving weakly bound  $^6\text{Li}$  and  $^{209}\text{Bi}$  at energies near the coulomb barrier. *Phys. Rev. C* **83**, 034616 (2011). [doi:  
https://doi.org/10.1103/PhysRevC.83.034616](https://doi.org/10.1103/PhysRevC.83.034616)

[50] L.C. Chamon, D. Pereira, M.S. Hussein et al., Nonlocal description of the nucleus-nucleus interaction. *Phys. Rev. Lett.* **79**, 5218–5221 (1997). [doi:  
https://doi.org/10.1103/PhysRevLett.79.5218](https://doi.org/10.1103/PhysRevLett.79.5218)

[51] J. Lubian, J.L. Ferreira, J. Rangel et al., Fusion processes in collisions of  $^6\text{Li}$  beams on heavy targets. *Phys. Rev. C* **105**, 054601 (2022).

[52] L.F. Canto, J. Lubian, P.R.S. Gomes et al., Continuum-continuum coupling and polarization potentials for weakly bound systems. *Phys. Rev. C* **80**, 047601 (2009).

[53] K.H. Maier, T. Nail, R.K. Sheline et al., Structure of  $^{209}\text{Bi}$  deduced from the  $^{208}\text{Pb}(t, 2n\gamma)$  reaction. *Phys. Rev. C* **27**, 1431–1453 (1983). [doi:  
https://doi.org/10.1103/PhysRevC.27.1431](https://doi.org/10.1103/PhysRevC.27.1431)

[54] NuShellX for Windows and Linux, <http://www.garsington.eclipse.co.uk/> (2024)

[55] E.K. Warburton, B.A. Brown, Appraisal of the kuo-herling shell-model interaction and application to  $a=210-212$  nuclei. *Phys. Rev. C* **43**, 602–617 (1991). [doi:  
https://doi.org/10.1103/PhysRevC.43.602](https://doi.org/10.1103/PhysRevC.43.602)

[56] J. McGrory, T. Kuo, Shell model calculations of two to four identical-“particle” systems near  $^{208}\text{Pb}$ . *Nucl. Phys. A* **247**, 283–316 (1975). [doi:  
https://doi.org/10.1016/0375-9474\(75\)90637-5](https://doi.org/10.1016/0375-9474(75)90637-5)